Uniformly Stable Parameterized Macromodeling through Positive Definite Basis Funtions

Uniformly Stable Parameterized Macromodeling through Positive Definite Basis Funtions

Alessandro Zanco, *Student Member, IEEE*, Stefano Grivet-Talocia, *Fellow, IEEE*, Tommaso Bradde, *Student Member, IEEE*, Marco De Stefano, *Student Member, IEEE*

***Abstract*—Reduced-order models are widely used to reduce the computational cost required by the numerical assessment of electrical performance during the design cycle of electronic circuits and systems. Although standard macromodeling algorithms can be considered to be well consolidated, the generation of macromodels that embed in a closed form some dependence on the design variables still presents considerable margins for improvement. One of these aspects is enforcement of uniform stability throughout the parameter space of interest. This paper proposes a novel parameterized macromodeling strategy, which enforces by construction that all macromodel poles are stable for any combination of possibly several independent design variables. The key enabling factor is adoption of positive definite multivariate basis functions for the representation of model variations induced by the parameters. This representation leads to robust model generation from tabulated frequency responses, at a computational cost that is dramatically reduced with respect to competing approaches. This result arises from a number of algebraic constraints for stability enforcement that depends on the model complexity (number of basis functions) and not on the model behavior as a function of the parameters. As a byproduct, the proposed strategy lends itself to much improved scaling with the dimension of parameter space, allowing to circumvent the curse of dimensionality that may occur when the number of independent parameters grows beyond few units. To this end, we exploit representations based on positive definite radial basis functions. The benefits of the proposed approach are demonstrated through an extensive experimental campaign applied to both passive and active devices and components, comparing the performance of different model parameterizations in terms of accuracy, time requirements and model compactness.**

I. Introduction

The focus of this paper is on generation of Linear and Time-Invariant (LTI) behavioral models of complex devices, circuits, structures or systems, whose frequency response depends on several independent parameters. We term these as *parameterized macromodels*. This paper builds on some existing and well-documented model structure, and proposes a few extensions that: i) enable generation of parameterized models using more robust algorithms in significantly shorter time; ii) guarantees uniform stability by construction (all model poles are stable for any parameter combination); and iii) enables scalability to significantly higher number of independent parameters with respect to state of the art algorithms.

There are several application scenarios that may benefit from the proposed methodology. All these scenarios share the common feature of one or more independent parameters that we want to embed in the model equations. These can be geometry, material, process, or even ambient parameters that induce some variation on the dynamic responses of the structure under investigation. Some of these parameters may be design variables to be optimized for performance, while some other parameters may be uncertain, so that compact behavioral models may help in sensitivity studies, or even to speed up Monte Carlo simulations [1]. We propose a general macromodeling strategy that is applicable to all these scenarios.

Concerning target structures, a first natural application for which proposed methodology is adequate involves electrical interconnects at any level of packaging, parameterized by geometrical and material variables. These are intrinsically passive LTI structures, for which behavioral macromodels are required in order to enable transient system-level simulations accounting for all parasitics and/or electromagnetic phenomena that are best described in the frequency-domain [2]–[6]. The same consideration applies also to integrated or discrete components such as inductors or capacitors, whose response may depend not only on geometry but also on temperature and even on biasing voltage/current, the latter to be considered as parameters. A further generalization in scope leads to consider active circuit blocks intended to operate under small-signal conditions in the neighborhood of some well-defined operating point. We include in this class Low Noise Amplifiers (LNAs), Low Drop-Out (LDO) voltage regulators, and similar structures [7]. In summary, the proposed parameterized macromodeling framework is applicable to any passive or active physical structure that can be represented as an input-output transfer function, which in addition to frequency depends on additional parameters.

The subject of macromodeling, including extension to the parameterized case is huge and growing. This subject is not only of interest for electrical, electronic, or electromagnetic communities, but also to wider multi- and cross-disciplinary fields. We refer the Reader to [6], [8] for a review. In this work, we focus on data-driven approaches, where macromodels are derived from tabulated frequency responses [9]–[12] (a straightforward extension would process time-domain responses, see e.g. [13]). This is complementary to those Model Order Reduction (MOR) approaches that construct macromodels through compression, projection or truncation of some pre-existing large-scale model [14]–[21]. The latter scenario is typical when one builds a detailed circuit model based on first-principle formulation and/or extraction, and then wants to reduce the complexity of this model to a size/order that is manageable in later system-level simulations. Recent advances in projection-based reduction of possibly active blocks with

guaranteed stability are documented in [22], [23], although extension to the general high-dimensional parameterized case is still an open problem.

This work builds on a number of pre-existing results. First, we exploit the so-called rational barycentric model structure, originally adopted for non-parameterized models [24] (see also [25]–[27]) and later extended to the parameterized case [28], [29]. Second we take advantage of passivity characterization results originated several decades ago from [30], then formalized in [31] and extended in [32]–[34] to general univariate models and [35], [36] to parameterized models. Finally, we exploit a set of known results on sufficient conditions for uniform model stability, first introduced in [37] and extended in [38]. Additional considerations on background material are provided in Sections II and III, where relevant literature is reviewed in the context of proposed framework.

The main extensions proposed in this work are based on

1) adopting a parameterized rational barycentric model structure in conjunction with positive semidefinite multivariate basis functions to represent the variations induced by the parameters;
2) casting constraints related to uniform stability in terms of model coefficients as opposed to model responses. This point is the key enabling factor for dramatic complexity reduction and improved scalability;
3) adopting mesh-free unstructured basis functions, in particular Radial Basis Functions (RBF) in the parameter space, in order to ensure better scalability to a large number of parameters.

Combining these three independent options allow us to perform a thorough experimental campaign, aimed at showing how the parameterization strategy may influence model compactness and generation runtime. Rather than proposing a particular "universal" solution, we compare different alternatives by providing guidelines for choosing a particular strategy and balancing model accuracy, runtime in model construction, and scalability to high dimension. In particular, we show that using Bernstein polynomials instead of the more standard Chebychev polynomials enables a dramatic reduction in model generation time when the number of parameters is limited, still retaining polynomial accuracy. We also demonstrate scalability to higher dimensions thanks to positive definite RBFs (extending the Gaussian RBFs used originally in [39]), which appear to be the only candidate for achieving uniform stability in high-dimensional parameter spaces.

A large set of numerical results, documented for more than ten different structures parameterized by up to ten independent variables (plus frequency), confirms that proposed framework has the potential to break the limits of current strategies, and to become the method of choice for parameterized macromodeling.

II. Background and Notation

In the following we will denote scalars with lowercase italic fonts x, vectors with lowercase bold fonts $\mathbf{x}$, and matrices with uppercase bold fonts $\mathbf{X}$. The transpose and the hermitian transpose of a given matrix $\mathbf{X}$ will be denoted as $\mathbf{X}^{\mathsf{T}}$ and $\mathbf{X}^{\mathsf{H}}$, with the corresponding eigenvalue and singular value spectra $\lambda(\mathbf{X})$ and $\sigma(\mathbf{X})$, respectively. The operators $\Re\{\}$ and $\Im\{\}$ extract the real and the imaginary parts of their complex argument, with * denoting complex conjugation. Unless otherwise noted, the upper limit for a generic index n is denoted with an overbar as $\bar{n}$.

We start by considering a generic P-port electric, electronic, or electromagnetic structure, whose behavior depends on a number ρ of independent parameters, collected in vector $\boldsymbol{\vartheta} = [\vartheta^1, \vartheta^2, ..., \vartheta^\rho]^{\mathsf{T}}$. Throughout this work, we will assume that these parameters can attain values within a ρ-dimensional hyper-rectangle $\Theta \subseteq \mathbb{R}^\rho$ defined as

$$\Theta = [\vartheta^1_{\min}, \vartheta^1_{\max}] \times [\vartheta^2_{\min}, \vartheta^2_{\max}] \times ... \times [\vartheta^\rho_{\min}, \vartheta^\rho_{\max}] \quad (1)$$

and denoted in the following as the *parameter space*.

It is assumed that the broadband dynamic behavior of the structure is known by means of physical or virtual measurements (i.e., numeric simulations) of its frequency response, performed at discrete frequency-parameter values $(\mathrm{j}\omega_k; \boldsymbol{\vartheta}_m)$ in a given electrical representation (e.g. scattering, impedance, admittance),

$$\breve{\mathbf{H}}_{k,m} = \breve{\mathbf{H}}(\mathrm{j}\omega_k; \boldsymbol{\vartheta}_m) \quad k = 1, ..., \bar{k}, \quad m = 1, .., \bar{m}. \quad (2)$$

If the structure is linear and passive, then $\breve{\mathbf{H}}(\mathrm{j}\omega; \boldsymbol{\vartheta})$ represents its transfer matrix in the adopted representation. In case of nonlinear and possibly active circuit blocks, we assume a well-defined operating point, and $\breve{\mathbf{H}}(\mathrm{j}\omega; \boldsymbol{\vartheta})$ is the corresponding small-signal response. Thus, the proposed framework is applicable only to linear or linearized models. The frequency band of interest $\Omega = [0, \omega_{\bar{k}}]$ is induced by the highest available frequency sample.

We aim at obtaining a reduced order model $\mathbf{H}(s; \boldsymbol{\vartheta})$ with a rational dependence on the complex frequency s, so that it can be synthesized as a set of parameterized Ordinary Differential Equations (ODE) in state-space form, or alternatively as a parameterized behavioral SPICE netlist, see [37] for details. Due to this requirement, we assume the following model structure

$$\mathbf{H}(s; \boldsymbol{\vartheta}) = \frac{\mathbf{N}(s; \boldsymbol{\vartheta})}{D(s; \boldsymbol{\vartheta})} = \sum_{n=0}^{\bar{n}} \frac{\mathbf{R}_n(\boldsymbol{\vartheta})}{s - p_n(\boldsymbol{\vartheta})} = \quad (3)$$
$$= \frac{\sum_{n=0}^{\bar{n}} \sum_{\ell=1}^{\bar{\ell}} \mathbf{R}_{n,\ell}\, \xi_\ell(\boldsymbol{\vartheta})\, \varphi_n(s)}{\sum_{n=0}^{\bar{n}} \sum_{\ell=1}^{\bar{\ell}} r_{n,\ell}\, \xi_\ell(\boldsymbol{\vartheta})\, \varphi_n(s)}.$$

The rational form of (3) is induced by the partial fraction basis $\varphi_0(s) = 1$, $\varphi_n(s) = (s - q_n)^{-1}$ where q_n are given stable "basis" poles, as in the Vector Fitting (VF) algorithm [40] (these basis poles are either real or appear in conjugate pairs: without loss of generality we assume here only real poles to simplify notation). The basis poles q_n are here predetermined by a non-parameterized pole relocation based on VF, applied to the data $\breve{\mathbf{H}}(\,\cdot\,; \boldsymbol{\vartheta}_{\mathrm{center}})$ where $\boldsymbol{\vartheta}_{\mathrm{center}}$ is the closest available parameter instance to the centroid of Θ.

The model structure (3) is based on a particular choice of multivariate basis functions $\xi_\ell(\boldsymbol{\vartheta}) : \Theta \to \mathbb{R}$, which are responsible for representing the variations induced by the design variables. In fact, this paper documents how the choice

of these basis functions may impact model robustness, complexity, scalability, efficiency in its construction, and especially uniform stability. The matrices $\mathbf{R}_{n,\ell} \in \mathbb{R}^{P\times P}$ and scalars $r_{n,\ell} \in \mathbb{R}$ are unknown coefficients. These are computed by enforcing the fitting condition

$$\mathbf{H}(\mathrm{j}\omega_k;\boldsymbol{\vartheta}_m) \approx \breve{\mathbf{H}}_{k,m} \quad \forall k,\, \forall m \in \mathcal{M}_t, \tag{4}$$

so that the model responses approximate the data (2) over the entire parameter space and throughout the frequency band of interest with a controlled error. The index set $\mathcal{M}_t$ collects the first $\bar{m}_t$ samples, denoted as *training* samples. These samples must be spread as uniformly as possible in the parameter space, so that data variability is captured and exploited in model construction. The remaining $\bar{m}_v = \bar{m} - \bar{m}_t$ samples are used for model self-validation.

Condition (4) is in fact a nonlinear fitting problem, which is here solved through the well-established linear relaxation process known as *Parameterized Sanathanan-Koerner* (PSK) iteration [28], [29], [41]. We recall for convenience that the PSK iteration solves a sequence of weighted least squares problems

$$\min \sum_{k=1}^{\bar{k}} \sum_{m\in\mathcal{M}_t} \left\| \frac{\mathbf{N}^{\mu}(\mathrm{j}\omega_k;\boldsymbol{\vartheta}_m) - D^{\mu}(\mathrm{j}\omega_k;\boldsymbol{\vartheta}_m)\breve{\mathbf{H}}_{k,m}}{D^{\mu-1}(\mathrm{j}\omega_k;\boldsymbol{\vartheta}_m)} \right\|_F^2 \tag{5}$$

through iterations $\mu = 1, 2, \ldots$, until the coefficients and the corresponding fitting error stabilize. This cost function can be generalized from the standard Frobenius norm $\|\cdot\|_F$ to more general application-specific choices, including relative or frequency-weighted model-data error definitions [6], [42].

The number $\bar{\ell}$ of multivariate basis functions is crucial for a successful model fitting. On one hand, $\bar{\ell}$ must be large enough so that the data variability is captured by the adopted basis set. On the other hand, $\bar{\ell}$ should not be too large to avoid overfitting. We avoid such condition by ensuring $\bar{\ell} \ll \bar{m}_t$, so that the least squares system originating from (5) is sufficiently overdetermined.

Some advanced adaptive algorithms exist (see [43] and references therein) for the automated and combined determination of both model order $\bar{\ell}$ and training samples $\bar{m}_t$. Such methods are only adequate for $\rho \leq 3$ due to curse of dimensionality and are therefore not used here. The actual order is here determined heuristically, by iteratively increasing the number of basis functions until the model accuracy is satisfactory. Should the number of training samples prove insufficient due to overfitting constraints, then $\bar{m}_t$ is increased iteratively by computing new samples

Before proceeding, we remark that our implementation considers a slightly more general model structure than (3), with different orders $\bar{\ell}_N$ and $\bar{\ell}_D$ for numerator and denominator, respectively.

III. Enforcing Uniform Stability

A. Uniform Stability

Stability is an essential quality that must be preserved whenever a macromodel is exploited in time domain simulations, although several methods have been proposed without considering stability, see e.g. the parameterized Loewner frameworks in [11], [12]. In our parameterized setting, this requirement translates into the enforcement of stability for any possible parameter values in the parameter space

$$\Re\{p_n(\boldsymbol{\vartheta})\} < 0 \quad \forall \boldsymbol{\vartheta} \in \Theta\,. \tag{6}$$

This property is here denoted as *uniform stability*.

In our proposed framework, the poles $p_n(\boldsymbol{\vartheta})$ are not directly available as decision variables during model construction, since they are only implicitly parameterized by the adopted model structure (3). Therefore, imposing uniform stability implies the definition and enforcement of dedicated constraints during the solution of (4) through (5). One of the main results of this work is a strategy to reduce the number and the complexity of such constraints, thanks to a careful choice of the multivariate basis functions $\xi_\ell(\boldsymbol{\vartheta})$.

B. Uniform Stability via Positive Interpolation

Over the last few years, a number of simplified approaches have been presented to enforce uniform stability of parameterized models by construction, without any requirement of numerical stability enforcement through constraints. For instance, the methods proposed in [**?**], [44]–[46] avoid the parameterization of the model poles through a model structure

$$\mathbf{H}(s;\boldsymbol{\vartheta}) = \sum_{\ell} \alpha_\ell(\boldsymbol{\vartheta})\mathbf{H}_\ell(s) \tag{7}$$

where $\mathbf{H}_\ell(s)$ are non-parameterized models constructed at each parameter data point $\boldsymbol{\vartheta}_\ell$, with $\alpha_\ell(\boldsymbol{\vartheta})$ being parameter-dependent interpolating kernels. If the individual submodels $\mathbf{H}_\ell(s)$ are stable (e.g., as obtained via VF pole relocation), then also the interpolated model $\mathbf{H}(s;\boldsymbol{\vartheta})$ is uniformly stable. This approach is extremely robust. However, the model poles are obtained as the union of all submodel poles, therefore the model complexity is much higher than required. In addition, the model poles are non-parameterized, as physical considerations would require, but only their residues (weights) are parameter-dependent.

The above limitations motivated various successive improvements. In [47], parameter-dependent frequency transformations were adopted to allow for smooth pole variations in the parameter space. A drawback of this approach is that pole trajectories may undergo bifurcations and are non-smooth in general, thereby making smoothness assumptions inadequate [48]. A further generalization based on state-space interpolation [49] in particular coordinate systems solved this problem while addressing also model redundancy. The latter approach in fact leads to a model structure that is very similar to (3) and practically coincides with (3) if the barycentric form is adopted, as advised in [49].

C. Sufficient Conditions for Uniform Stability

Assuming model structure (3), the direct enforcement of condition (6) is not straightforward. Although a-posteriori purely algebraic uniform stability checks based on the feasibility of a set of Lyapunov equations have been proposed [29] for the particular case of PieceWise Linear (PWL) basis

functions $\xi_\ell(\boldsymbol{\vartheta})$, general a-priori conditions that are equivalent to uniform stability of (3) are not available.

The above problems motivated the introduction of some level of conservativism in the uniform stability enforcement. It was shown in [37] that if the denominator $D(s,\boldsymbol{\vartheta})$ is a (strictly) Positive Real (PR) function, which in our setting reduces to condition

$$\Re\{D(s,\boldsymbol{\vartheta})\} > \gamma \quad \Re\{s\} > 0,\ \forall \boldsymbol{\vartheta} \in \Theta \tag{8}$$

for a given strictly positive constant $\gamma > 0$, then (6) holds, and the model is uniformly stable. The numerical implementation of (8) requires a careful selection of frequency-parameter points $(\mathrm{j}\hat{\omega}_k, \hat{\boldsymbol{\vartheta}}_m)$ where (8) is discretized as

$$\Re\left\{\sum_{n=0}^{\bar{n}}\sum_{\ell=1}^{\bar{\ell}} r_{n,\ell}\,\xi_\ell(\hat{\boldsymbol{\vartheta}}_m)\,\varphi_n(\mathrm{j}\hat{\omega}_k)\right\} > \gamma > 0 \tag{9}$$

and enforced in combination with (5). The most straightforward approach is to select the points $(\mathrm{j}\hat{\omega}_k, \hat{\boldsymbol{\vartheta}}_m)$ where PR constraints are enforced as a dense uniform grid in $\Omega \times \Theta$. This strategy is however problematic, since

- it does not guarantee not to miss localized regions where $D(s,\boldsymbol{\vartheta})$ is not PR;
- it may lead to a very large number of constraints, whose complexity blows up when the number of parameters ρ increases beyond few units.

D. Uniform Stability via Adaptive Sampling

The above problems were addressed in [37], where an adaptive sampling strategy in the parameter space was introduced in order to limit the number of constraints (9). Noting that the PR condition (8) is equivalent to requiring that the denominator function $D(s,\boldsymbol{\vartheta})$ represents a passive immittance submodel [50], [51], algebraic conditions based on Hamiltonian eigenvalue perturbation were applied for checking the passivity of $D(s,\boldsymbol{\vartheta})$ during model construction, and the corresponding results were used to drive an adaptive sampling based on structured mesh refinement in the parameter space, in order to spot all regions in Θ where the real part $D(s,\boldsymbol{\vartheta})$ is negative. Placing PR constraints in these regions leads to iterative optimization of model coefficients towards elimination of such regions. An example is reported in Fig. 1, where the automatically determined points in a 2D parameter space are depicted with a red or green color to denote a locally unstable or stable model. A more detailed description of the adaptive sampling algorithm can be found in [36].

The above adaptive sampling strategy is feasible for up to $\rho = 3$ parameters at most, since the computational cost for the formulation of the constraints still scales exponentially with ρ. This is mainly due to the fact that

- the location of these constraints depends on the model (denominator) response while this is being computed through iterations, and this response is defined over a compact set Θ with dimension ρ, which needs to be scanned for all regions where the real part of $D(s,\boldsymbol{\vartheta})$ is negative;
- the adaptive refinement is based on structured subgridding, with a number of points that inevitably scales exponentially with ρ.

Therefore, this method is definitely not adequate for applications where the number of design parameters is medium or large. This is the main problem we intend to overcome in this work, as documented in Section IV.

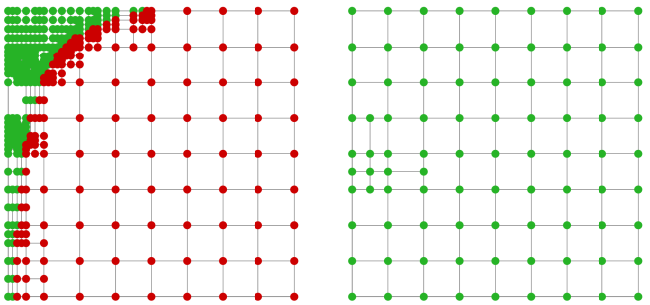

Fig. 1. Adaptive sampling of a 2D parameter space at two successive PSK iterations. Red and green dots denote, respectively, locally unstable and stable parameter combinations. Left panel: residual local unstable parameter combinations are present during iteration. Right panel: uniformly stable macromodel obtained by adding uniform stability constraints at locally unstable parameter points.

IV. Beyond Sampling Techniques

The key factor enabling to break the curse of dimensionality implied by the above-described dense or adaptive sampling techniques is to formulate PR constraints directly on the model *structure* rather than on the *response* (of the denominator, in our setting). In order to achieve this goal, we exploit the degrees of freedom that we have in the selection of the parameter-dependent basis functions $\xi_\ell(\boldsymbol{\vartheta})$.

Up to now, we have not discussed in detail which basis functions should be adopted to represent parameter variations. Several previous publications were based on polynomial bases, either monomials or orthogonal polynomials for improved numerical conditioning, see e.g. [28], [29]. The most common choice is multivariate Chebychev polynomials obtained as cartesian products of univariate Chebychev polynomial bases, one for each dimension of the parameter space [36], [37]. Defining $\xi_\ell(\boldsymbol{\vartheta})$ as polynomials has the additional advantage that the response of any lumped circuit is represented *exactly* by a first-order (multi-affine) polynomial expansion of both numerator and denominator as in (3), see [52], [53]. Therefore, using higher-order polynomials seems to be a natural extension to handle electromagnetic (distributed) structures or linearized small-signal models of nonlinear active circuit blocks. The standard multivariate Chebychev polynomials will be used in this work as a benchmark representation, in order to illustrate the improvements that can be enabled by using positive definite basis functions.

Based on the preliminary results in [39], we assume in the following that the basis functions $\xi_\ell(\boldsymbol{\vartheta})$ are positive semi-definite

$$\xi_\ell(\boldsymbol{\vartheta}) \geq 0, \quad \forall \ell,\ \forall \boldsymbol{\vartheta} \in \Theta. \tag{10}$$

With this additional property, the positive realness of $D(s,\boldsymbol{\vartheta})$ can be shown to be implied by a set of discrete conditions applied directly on the denominator coefficients $r_{n,\ell}$. To prove this statement, we first rewrite $D(s,\boldsymbol{\vartheta})$ by splitting the contribution of the $\bar{n}_r$ real poles q_n with coefficients $r_{n,\ell}$ and $2\cdot\bar{n}_c$ complex poles $\alpha_n \pm \mathrm{j}\beta_n$ with coefficients $r'_{n,\ell} \pm \mathrm{j}r''_{n,\ell}$. We obtain

$$D(s,\boldsymbol{\vartheta}) = \sum_{n=0}^{\bar{n}_r}\sum_{\ell=1}^{\bar{\ell}} \frac{r_{n,\ell}}{s-q_n}\xi_\ell(\boldsymbol{\vartheta}) + \sum_{n=0}^{\bar{n}_c}\sum_{\ell=1}^{\bar{\ell}} \left[\frac{r'_{n,\ell}+\mathrm{j}r''_{n,\ell}}{s-\alpha_n-\mathrm{j}\beta_n} + \frac{r'_{n,\ell}-\mathrm{j}r''_{n,\ell}}{s-\alpha_n+\mathrm{j}\beta_n}\right]\xi_\ell(\boldsymbol{\vartheta}). \tag{11}$$

Provided that all basis poles are strictly stable, with $q_n<0$ and $\alpha_n<0$, enforcing that the real part of each contribution in (11) is nonnegative leads to the following algebraic conditions

$$\begin{cases} r_{n,\ell} > 0 \\ -\alpha_n\cdot r'_{n,\ell} \pm \beta_n \cdot r''_{n,\ell} > 0 \end{cases} \tag{12}$$

arising from real and complex pairs, respectively. These conditions, proved in Appendix A, are thus sufficient to guarantee that the real part of $D(s,\boldsymbol{\vartheta})$ is also nonnegative, as a superposition of nonnegative terms [54]. In case strict positivity is desired, as required by (8), we have the more stringent conditions

$$\begin{cases} r_{n,\ell} > \gamma_r \\ -\alpha_n\cdot r'_{n,\ell} \pm \beta_n \cdot r''_{n,\ell} > \gamma_c \end{cases} \tag{13}$$

where $\gamma_r>0$ and $\gamma_c>0$ are arbitrary positive constants.

As a result, uniform stability constraints to be enforced with (5) can be formulated directly in terms of the model coefficients as in (13). The number of such constraints, which depends on the model structure and not on the model response, is known in advance and matches the total number of basis functions $(\bar{n}+1)\bar{\ell}$. Moreover, no dense or adaptive sampling is required in a possibily high-dimensional parameter space. The drawback underlying this formulation is the increased degree of conservativism, since (13) provide only sufficient but not necessary conditions for the positive realness of $D(s,\boldsymbol{\vartheta})$. Therefore, a somewhat reduced accuracy of the final model responses with respect to the traning data samples is to be expected.

V. Choosing Positive Definite Bases

A. Bernstein Polynomials

Bernstein polynomials have been widely used in polynomial approximation as they are capable to uniformly approximating continuous functions over a prescribed interval [55]. Given a maximum degree $\bar{\nu}$, the Bernstein polynomials $b_{\nu,\bar{\nu}}(x)$ in the scalar normalized variable $x\in[0,1]$ are defined as

$$b_{\nu,\bar{\nu}}(x) = \binom{\bar{\nu}}{\nu} x^\nu (1-x)^{\bar{\nu}-\nu}, \quad \nu=0,\dots,\bar{\nu}. \tag{14}$$

These polynomials are strictly positive in their normalized domain $[0,1]$, with the exception of the two zeros of order ν and $\bar{\nu}-\nu$ and at the edges $x=0$ and $x=1$, see Fig. 2. As the index ν increases, the *localization* of the corresponding polynomials shifts from the left to the right edge of the domain, a fact that has been exploited in many application fields, from computer graphics [56] down to the construction of biorthogonal hierarchical wavelet bases with optimal localization [57]. These characteristics make Bernstein polynomials excellent candidates for parameterized macro-modeling with uniform stability constraints, since positivity of a Bernstein polynomial approximation is implied by positivity of the corresponding coefficients

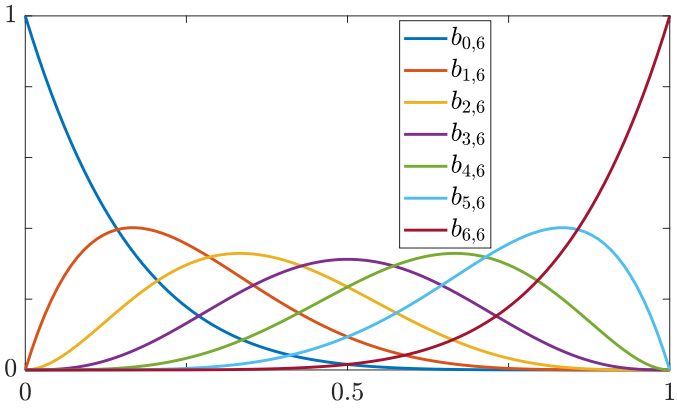

Fig. 2. Bernstein polynomials $b_{\nu,6}(x)$, for $\nu=0,\dots,6$.

$$\sum_{\nu=0}^{\bar{\nu}} c_\nu b_{\nu,\bar{\nu}}(x) > 0,\ \forall x \quad \Longleftarrow \quad c_\nu > 0,\ \forall \nu. \tag{15}$$

We then define the set of parameter-dependent basis functions $\xi_\ell(\boldsymbol{\vartheta})$ as the Cartesian product of univariate Bernstein polynomials

$$\xi_\ell(\boldsymbol{\vartheta}) = \prod_{i=1}^{\rho} \xi_{\ell_i}(\vartheta_i), \quad \xi_{\ell_i}(\vartheta_i) = b_{\ell_i,\bar{\ell}_i}(\vartheta_i) \tag{16}$$

where index ℓ_i refers to the i-th coordinate in the parameter space, and ℓ is a global linear index spanning the multivariate basis of size $\bar{\ell}=\prod_i(1+\bar{\ell}_i)$. A few remarks are in order.

- Given a polynomial degree $\bar{\ell}_i$ for each i-th coordinate, the approximation space provided by the Bernstein polynomial basis is identical to the space provided by any different polynomial basis with the same degree, including monomials and Chebychev bases. Therefore, up to differences in approximation errors due to the different numerical conditioning properties of the bases, we expect identical results if the same model generation algorithm is run with the same data and different polynomial bases.
- Being positive definite, the Bernstein polynomials allow for uniform stability enforcement through constraints (13), which are incompatible, e.g., with Chebychev polynomials.
- Being structured as a Cartesian product of univariate polynomial bases, Bernstein polynomials cannot be adopted when the number of parameters ρ is large, due to curse of dimensionality.

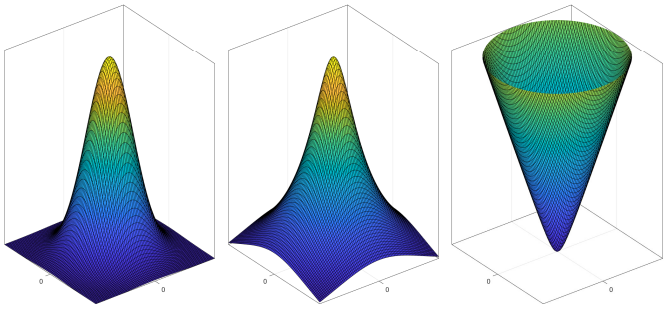

Fig. 3. Three radial basis functions tested in this work, depicted in a 2D domain. From left to right: gaussian RBF, inverse multiquadric RBF, multiquadric RBF.

B. Radial Basis Functions

A possible approach for breaking complexity in both model representation and numerical construction when ρ increases, is to adopt mesh-free unstructured bases, such as Radial Basis Functions (RBF) [58]. Kernel-based approximation methods [59], and in particular, RBF-based expansions [60], gained widespread popularity due to their excellent capabilities in reconstructing an unknown multivariate function from a reduced set of known scattered data. A function $\Phi_{\mathbf{x}_0}(\mathbf{x}) : \mathbb{R}^\rho \to \mathbb{R}$ is defined *radial* if its value depends only on the distance of $\mathbf{x}$ with respect to a symmetry center $\mathbf{x}_0 \in \mathbb{R}^\rho$, as

$$\Phi_{\mathbf{x}_0}(\mathbf{x}) = \Phi(\mathbf{x} - \mathbf{x}_0) = \varphi(\|\mathbf{x} - \mathbf{x}_0\|), \ \forall \mathbf{x}_0. \tag{17}$$

Although $\|\cdot\|$ may be any vector norm, in this work it is intended as the Euclidean norm.

The possibility of arbitrarily selecting a center $\mathbf{x}_0$ makes RBFs excellent candidates to approximate multivariate functions based on even irregularly positioned training data points. Even though RBFs are defined over a possibly high-dimensional domain, their argument reduces to the scalar quantity $\|\mathbf{x} - \mathbf{x}_0\|$. Therefore, the number of RBFs required to construct an approximation is not related to the size of the embedding space, but only to the variations of the target function within its domain. Preliminary results on RBF-based parameterized macromodels [39] already pointed that the complexity of RBF approximations increases only linearly with the parameter space dimension ρ, whereas scalability with tensor-product polynomials is exponential, thus unsuitable for large ρ.

Thanks to their favorable numerical properties and suitability for proposed uniform stability enforcement, we consider here only positive definite RBFs, characterized by $\Phi(\mathbf{x}) > 0, \ \forall \mathbf{x} \in \mathbb{R}^\rho$. Among the many alternatives, this work documents tests based on the follwing three RBF classes (see Fig. 3 for an illustration and [58] for a general introduction)

1) Gaussian: $\Phi_{\mathbf{x}_0;\varepsilon}(\mathbf{x}) = e^{-\varepsilon\|\mathbf{x}-\mathbf{x}_0\|^2}$
2) Multiquadric: $\Phi_{\mathbf{x}_0;\varepsilon}(\mathbf{x}) = (\|\mathbf{x} - \mathbf{x}_0\|^2 + \varepsilon^2)^{1/2}$
3) Inverse multiquadric: $\Phi_{\mathbf{x}_0;\varepsilon}(\mathbf{x}) = (\|\mathbf{x} - \mathbf{x}_0\|^2 + \varepsilon^2)^{-1/2}$

where ε is a free hyper-parameter, defined also as *shape parameter*, that determines the RBFs smoothness (equivalently, "size" or "width"). The optimal choice of such hyper-parameter is still an open problem, and usually the best ε is determined through some additional optimization [61]. All results in this work were obtained by determining the optimal ε for any given RBF class through a basic parameter sweep.

For any given RBF class, we define our parameterized macromodel structure as in (3), with

$$\xi_\ell(\boldsymbol{\vartheta}) = \Phi_{\mathring{\boldsymbol{\vartheta}}_\ell;\varepsilon}(\boldsymbol{\vartheta}) \tag{18}$$

where $\mathring{\boldsymbol{\vartheta}}_\ell$ denotes the center where the ℓ-th RBF is placed. The selection of these centers once the basis size $\bar{\ell}$ is fixed provides additional degrees of freedom to optimize model accuracy. In this work, we consider as candidate points a subset of the available data points for training, e.g.,

$$\{\mathring{\boldsymbol{\vartheta}}_\ell\}_{\ell=1}^{\bar{\ell}} \subseteq \{\boldsymbol{\vartheta}_m, \ m \in \mathcal{M}_t\}. \tag{19}$$

The actual subset set of centers is here determined randomly from the available data points. Despite this simplistic approach, the results provided in next section will show a remarkable accuracy for all investigated test cases. Therefore, even without advanced optimization of hyperparameters and distribution of RBF centers, this paper shows that naive and simple to implement solutions already provide excellent results and clear improvements with respect to the state of the art.

VI. Numerical Examples

A. Comparing performance of different basis functions

In this section, we present an extensive set of numerical results, with the aim of comparing the performance of the various parameterization schemes discussed in this work, and specifically to illustrate the advantages of positive definite bases in the enforcement of uniform stability.

A benchmark suite of ten different structures was constructed, as detailed in Table I. Structures numbered 1–5 depend on $\rho = 2$ parameters, whereas structures 6–10 depend on $\rho = 3$ parameters. These small-size parameter spaces allow for model construction using all presented approaches, including the standard polynomial approximation based on Cartesian product of univariate (Chebychev) polynomials, to be considered as a reference. The ten structures include both linearized active circuit blocks (1–6) and passive interconnects (7–10). Table I reports details on structure type, individual parameters with their range, and reference to the literature where additional information on each example can be retrieved.

For each of the structures listed in Table I, we derived uniformly stable parameterized macromodels in the form (3) making use of 5 different basis functions $\xi_\ell(\boldsymbol{\vartheta})$:

- multivariate Chebychev polynomials, for which uniform stability was enforced through iterative adaptive sampling, as discussed in Sec. III-D;
- multivariate Bernstein polynomials, with uniform stability enforced through constraints (13);
- Gaussian RBFs with constraints (13);
- Multiquadric RBFs with constraints (13);
- Inverse multiquadric RBFs with constraints (13).

We evaluate the quality of the resulting macromodels by means of three different metrics.

- The *Extraction Runtime* is the time required to solve 10 times the weighted least square problem (5) subject to the

TABLE I

BENCHMARK SUITE USED FOR THE COMPARATIVE STUDY OF DIFFERENT PARAMETERIZATION SCHEMES. FOR EACH TEST CASE 1–10 THE TABLE REPORTS DATASET INFORMATION AS: THE NUMBER OF PARAMETERS ρ, THE TOTAL NUMBER OF FREQUENCY SAMPLES $\bar{k}$ FOR EACH OF THE $\bar{m}$ AVAILABLE PARAMETRIC RESPONSES, AND DETAILS ON STRUCTURE TYPE, INDIVIDUAL PARAMETERS WITH THEIR RANGE, AND REFERENCES FOR ADDITIONAL INFO.

#	ρ	k	$\bar{m}$	Type	Parameters	Range
1	2	273	341	Buffer [7]	Bias voltage (V)	$[0.5,\ 1.5]$
					Temperature ($^\circ C$)	$[20,\ 50]$
2	2	293	231	Buffer [7]	Bias voltage (V)	$[0.5,\ 1.5]$
					Temperature ($^\circ C$)	$[20,\ 40]$
3	2	213	119	LNA [7]	Bias voltage (V)	$[0.9,\ 1.2]$
					Temperature ($^\circ C$)	$[-30,\ 130]$
4	2	235	35	LNA [7]	Bias voltage (V)	$[0.9,\ 1.2]$
					Input Voltage (V)	$[0.4,\ 0.6]$
5	2	210	231	OpAmp [62]	Bias voltage (V)	$[1.1,\ 1.3]$
					Gain	$[1.01,\ 2]$
6	3	831	935	OpAmp [62]	Bias voltage (V)	$[1.1,\ 1.3]$
					Temperature ($^\circ C$)	$[-30,\ 130]$
					Gain	$[1.01,\ 2]$
7	3	901	300	TL network [63]	Inductance (nH)	$[4.5,\ 5.5]$
					Inductance (nH)	$[9,\ 11]$
					Capacitance (pF)	$[0.9,\ 1.1]$
8	3	901	300	TL network [63]	Inductance (nH)	$[9,\ 11]$
					Capacitance (pF)	$[0.45,\ 0.55]$
					Resistance (Ω)	$[45,\ 55]$
9	3	901	300	TL network [63]	Inductance (nH)	$[9,\ 11]$
					Resistance (Ω)	$[45,\ 55]$
					Conductor width (μm)	$[90,\ 210]$
10	3	2000	216	TL filter [36]	Stub length (mm)	$[6,\ 7]$
					Line length (mm)	$[9,\ 10]$
					Load Γ	$[0.1,\ 0.5]$

stability constraints, necessary to generate the uniformly stable macromodels.

- The *Model Complexity*, measured in terms of the total number of free coefficients that are optimized during model-data fitting.
- The *Model Accuracy*, evaluated in terms of the achieved Root Mean Square (RMS) absolute error between model responses and data.

In order to gain better insight, we carried out two series of experiments.

1) A first set of models were generated by fixing the same complexity for all basis function choices, with the objective of comparing the achievable accuracy using the various parameterization schemes and associated constraints for stability enforcement.
2) A second set of models were obtained by setting a fixed target accuracy $\delta = 0.01$ in terms of worst-case RMS error, which can be considered to be an acceptable engineering accuracy. The model complexity was therefore tuned for each individual test case to achieve this precision.

The results of the experiments perfomed by fixing the model complexity are reported in panels (a) and (c) of Fig. 4 for cases 1–5 and 6–10, respectively. The fixed model complexity was predetermined so that all bases could achieve an acceptable accuracy. Only three structures (3,9,10) resulted in errors larger than 0.01 with multiquadric or inverse multiquadric RBFs, but only by a negligible amount. As expected, the Chebychev basis is the most accurate (subpanels a.1 and c.1), since the implementation of the uniform stability constraints through adaptive sampling is less conservative than for the other bases. This better accuracy comes with an increased cost in terms of runtime, which becomes impractical for the three-dimensional cases (subpanel c.3). Even for the low-complexity two-dimensional cases, the runtime required for model construction with standard Chebychev bases exceeds all other cases by one order of magnitude (subpanel a.3). This first set of examples shows that, at a moderate loss in accuracy, the computational cost for model construction is dramatically reduced with proposed stability enforcement framework based on positive definite bases.

Panels (b) and (d) of Fig. 4 report the results obtained by setting target model accuracy to $\delta = 0.01$. Also in this scenario the results confirm that model extraction runtime is dramatically reduced with positive definite bases with respect to Chebychev polynomials (subpanels b.3 and d.3). When increasing number of parameters, we also see that the number of coefficients defining model complexity is reduced when using mesh-free RBFs, compared to structured bases defined by Cartesian product of polynomials (subpanels b.2 and especially d.2). This improvement appears to be moderate for small ρ, as in this case, but it becomes dramatic for larger ρ (see next Sections), for which unstructured RBFs appear to be the only viable choice for model parameterization.

B. Operational amplifier

This example describes in details one of the models presented in benchmark suite of Section VI-A, in particular test case #6. The structure under modeling is a 3-port operational amplifier circuit block (originally presented in [62]), parameterized by its bias voltage $V_{\rm dd} \in [1.1,\ 1.3]V$, the operating temperature $T \in [-30,\ 130]\ ^\circ C$ and its gain

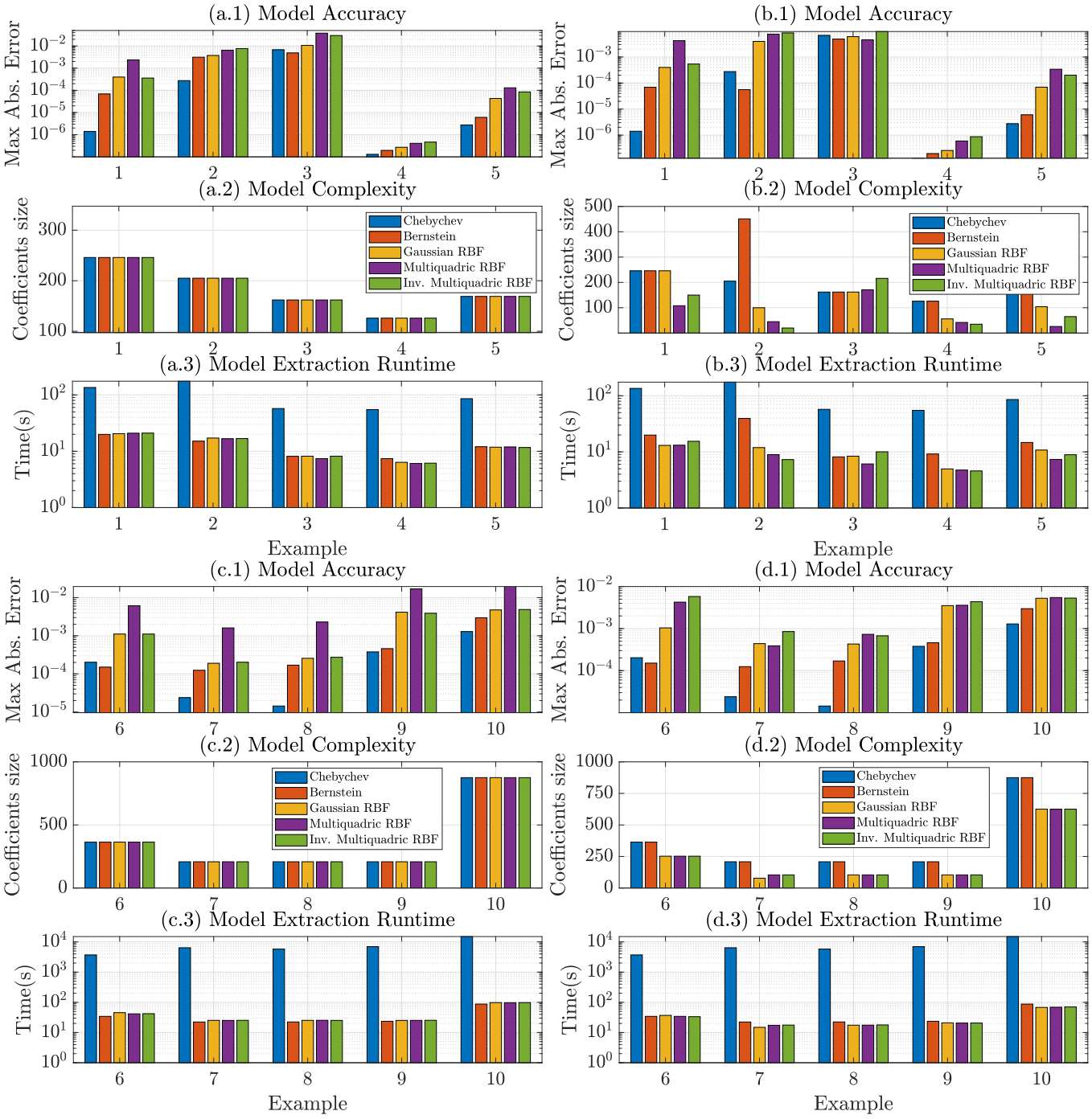

Fig. 4. Performance comparison of different parameterizations for ten benchmark structures: cases 1–5 (panels a, b) with $\rho = 2$ parameters, and 6–10 (panels c, d) with $\rho = 3$ parameters. Subpanels (a.i) and (c.i) for $i = 1, 2, 3$ compare performance in terms of model accuracy, complexity and runtime with a fixed total number of model coefficients for each individual example. Subpanels (b.i) and (d.i) show results obtained by tuning model complexity so that a prescribed model accuracy is attained.

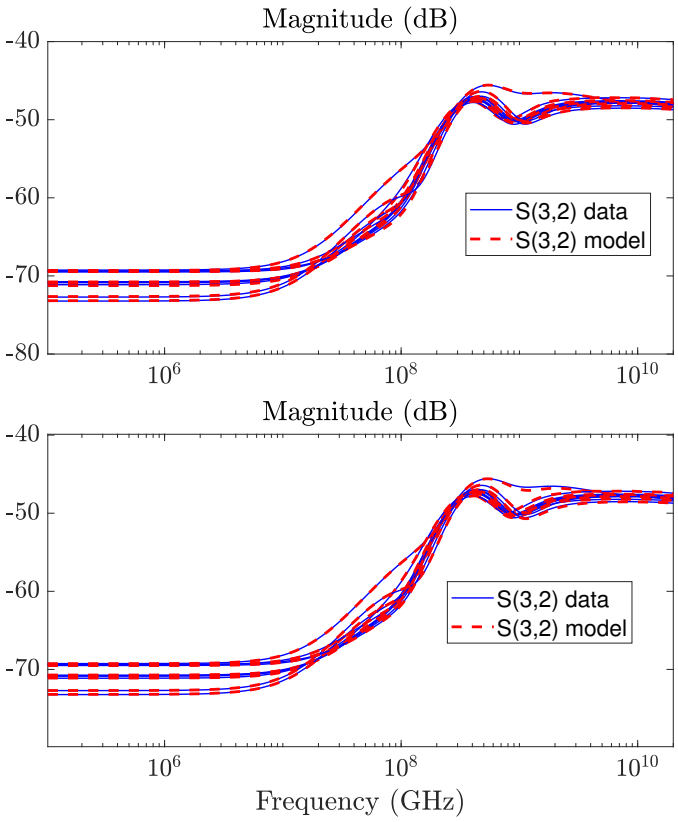

Fig. 5. Model responses compared with validation data for the operational amplifier circuit block. Top panel: model with Bernstein basis functions. Bottom panel: model with RBF basis functions.

$G \in [1.01,\ 2]$. The structure is characterized by a dataset of $\bar{m} = 935$ small-signal scattering responses, arranged on a 3-dimensional cartesian grid, ranging from 0.1 MHz to 20 GHz. Among all these responses, one half was used to construct the macromodels, leaving the other half for model validation.

We consider two models based on Bernstein and Gaussian RBF parameterization. Both models have been extracted with $\bar{n} = 18$ poles and are uniformly stable thanks to the adopted positive definite parameterization. The RBF model is constructed with $\bar{\ell} = 35$ RBFs for the numerator and $\bar{\ell} = 10$ for the denominator. The Bernstein polynomial model, which is based on a Cartesian product of univariate Bernstein polynomial bases, is defined with orders $\bar{\ell}_1 = 2$, $\bar{\ell}_2 = 1$, $\bar{\ell}_3 = 2$ for the three parameters, for both numerator and denominator.

Figure 5 compares the model responses with a randomly chosen subset of validation data for both Bernstein model (top panel) and RBF model (bottom panel). The Bernstein-based model has a worst-case absolute RMS error of $2.87 \cdot 10^{-3}$ while the RBF-based model has a worst-case absolute RMS error of $5.87 \cdot 10^{-3}$, both evaluated on validation samples. These results confirm that both bases are able to produce accurate uniformly stable macromodels, despite the additional degree of conservativism induced by the algebraic stability constraints (13).

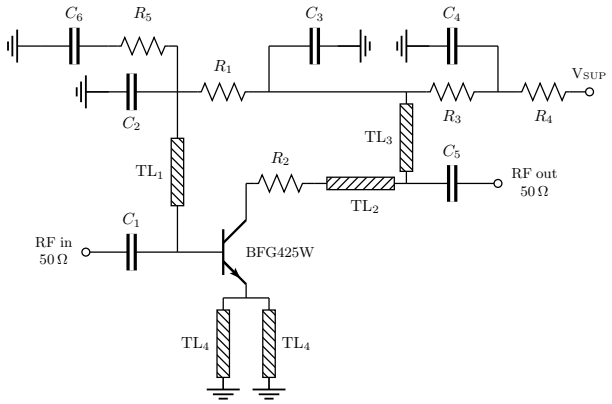

Fig. 6. A Low Noise Amplifier circuit [64].

C. Low Noise Amplifier

In this example, we show how the proposed approach can be exploited to derive compact parameterized macromodels of mixed lumped-distributed active circuit blocks. We consider the LNA structure shown in Fig. 6, first presented in [64]. We are interested in a behavioral small-signal scattering macromodel for the two-port circuit block, where the first port is the RF input, the second is the RF output. The bandwidth Ω of interest is $1-10$ GHz. The structure is parameterized by ten different and independent parameters (listed in Table II), six of which are lumped components (parasitic series inductances and shunt capacitances of the transistor). The other four are related to transmission line geometrical parameters.

Since the parameter space Θ has dimension $\rho = 10$, sparsity is required also in the extraction of the training data samples to be used for computing the model. This dataset was obtained by a set of small-signal SPICE simulations, each providing a total of $\bar{k} = 701$ linearly spaced samples in the range $1 - 10$ GHz. A total of $\bar{m} = 2000$ of such frequency responses were generated according to a *Latin Hypercube* distribution in the parameter space [65]. Latin Hypercube-based sampling have, roughly speaking, the property of uniformly filling the available space. Thus, they are good candidates for generating high-dimensional parametric datasets. Among all the available samples, only $\bar{m}_t = 160$ (randomly selected) responses were used for model generation, while the others were left for model validation.

For this high-dimensional test case, only RBF-based parameterizations are feasible within the proposed uniformly stable modeling framework. We document results based on Gaussian RBFs, with a common shape parameter $\varepsilon = 0.03$. The computed model has $\bar{n} = 16$ poles, with basis poles q_n determined through a preprocessing VF run, with a parameterization induced by $\bar{\ell} = 90$ for the numerator and $\bar{\ell} = 5$ for the denominator. Model extraction time was 91 seconds, requiring only 4 iterations to reach PSK convergence. The worst case RMS absolute error of the model with respect to the available validation samples is $7.72 \cdot 10^{-3}$, which is remarkable given the very small number of coefficients compares to the size of the parameter space. This accuracy is confirmed by Fig. 7, which compares a set of randomly selected parameterized

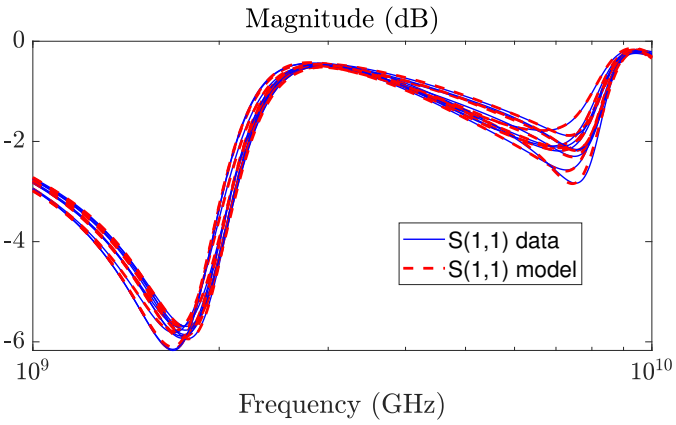

Fig. 7. Comparison of LNA model responses to corresponding raw validation responses, randomly selected in the 10-dimensional parameter space.

model responses to the corresponding validation data.

TABLE II
LNA PARAMETERS. FIRST SIX PARAMETERS: PARASITIC INDUCTANCES AND CAPACITANCES OF THE TRANSISTOR. THE REMAINING PARAMETERS ARE SUBSTRATE THICKNESS, CONDUCTOR THICKNESS, CONDUCTOR WIDTH FOR LINES TL_1, TL_2, TL_3 AND CONDUCTOR WIDTH FOR LINE TL_4.

#	Parameter ϑ_i	$\vartheta_{i,\min}$	$\vartheta_{i,\max}$
1	L_b (nH)	0.88	1.32
2	L_c (nH)	0.88	1.32
3	L_e (nH)	0.20	0.30
4	C_{cb} (pF)	0.0016	0.0024
5	C_{be} (pF)	0.064	0.096
6	C_{ce} (pF)	0.064	0.096
7	h (mm)	0.45	0.55
8	t_k (μm)	1.8	2.2
9	$w_{1,2,3}$ (mm)	0.225	0.275
10	w_4 (mm)	0.72	0.88

D. Scalability

In this example, we show the influence of the parameter space dimension ρ on model accuracy and especially complexity, by performing a scalability study. We consider the LNA circuit block already discussed in Sec. VI-C, and we increase the number of parameters from $\rho = 1$ up to $\rho = 10$, by adding one parameter at the time from the list in Table II. For each instance with fixed ρ, a dedicated set of training responses was obtained through repeated SPICE runs, based on a Latin Hypercube distribution. The total number of frequency responses was predefined as $M_\rho = 200\,\rho$, with a linear scaling law with the parameter space dimension. The numerical results that follow confirm that this number is sufficient to capture the variation induced by all parameters, up to $\rho = 10$. Note that if a uniform sampling were adopted, scalability in the number of responses would have been exponential, thus impractical.

A uniformly stable parameterized macromodel of each dataset was created using both Bernstein polynomials and Gaussian RBFs, which appear to provide the best performance among the tested RBFs according to the comparison of Fig. 4. For this investigation, the dynamic order was set to $\bar{n} = 16$ in all cases, and the model complexity was tuned in order to reach a target accuracy of $\delta = 0.01$ on the RMS absolute error. A common value of the shape parameter $\varepsilon = 0.03$ was set for all the Gaussian basis functions.

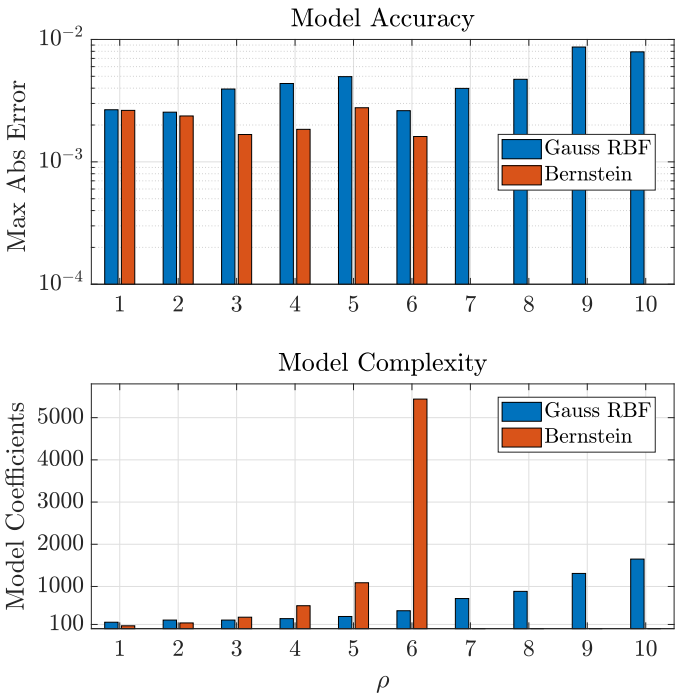

Fig. 8. Model accuracy and complexity of the LNA example obtained using Bernstein polynomials and Gaussian RBFs, for increasing parameter space dimension ρ.

TABLE III
MAIN FEATURES OF CONSIDERED PARAMETERIZATION STRATEGIES IN TERMS OF EXTRACTION RUNTIME, MODEL COMPACTNESS AND ACCURACY.

	Runtime	Compactness	Accuracy
Structured Unsigned	BAD	BAD	GOOD
Structured Positive	GOOD	BAD	MEDIUM
Unstructured Positive	GOOD	GOOD	MEDIUM

Figure 8 shows the scalability results in terms of model accuracy and complexity. Bernstein polynomials allow the generation of macromodels up to $\rho = 6$, due to an exponential growth of model complexity that prevents applicability for higher dimensions. As already noted, Gaussian-based models show a slight degradation of accuracy in some of the cases, although in all cases the achieved accuracy was better than the prescribed threshold. The main advantage of Gaussian RBF parameterization is evident from the bottom panel of Fig. 8, which shows a linear increase in model complexity when increasing ρ. These results confirm that mesh-free RBF representations are good candidate for high-dimensional parameterization, and that proposed framework is able to extract parameterized macromodels with excellent scalability.

E. Summary

The previous results suggest that there is not a well-defined and universal strategy in devising a parameterized model structure. The best choice depends on the particular application and structure at hand, resulting from a compromise between conflicting requirements. Table III summarizes the performance of the considered parameterization schemes in terms of extraction runtime, model compactness and accuracy. The results support the following conclusions

- Structured (polynomial) basis functions without sign constraints (e.g. Chebychev polynomials) appear to be the right choice only when a high accuracy is required (relative error below 10^{-2}) with few parameters (up to three at most). The drawback is a possibly large computational runtime.
- Constraining the structured basis to be positive definite (e.g., Bernstein) polynomials leads to a dramatic reduction of the extraction runtime, at a cost of a slight degradation of accuracy. The number of parameters this parameterization can handle is a bit larger, but still small (up to five-six).
- Mesh-free positive definite basis functions (RBFs) provide the only viable choice for uniformly stable models with a large number of independent parameters. Overall accuracy will depend in this case on the number of basis functions required to fit the data variability over the parameter space.

VII. Conclusions

This paper presented a framework for the construction of parameterized macromodels of passive or linearized active multiport structures. The main improvements with respect to the state of the art are enabled by adoption of positive definite multivariate bases to construct approximations in the parameter space. As a result, the proposed algorithms are able to enforce uniform stability of the macromodels through simple algebraic constraints on the model coefficients, without the need of time-consuming adaptive sampling loops. When mesh-free unstructured bases are chosen, such as Radial Basis Functions (RBF), it becomes possible to scale model complexity to higher parameter dimensions, thus circumventing the problem of curse of dimensionality. These improvements have been demonstrated with a thorough campaign of numerical simulations on several test cases. Numerical examples demonstrate feasibility up to ten independent parameters.

There are several aspects of proposed framework that deserve further investigations, specifically on the definition of the individual RBF components that construct the model parameterization. Optimization of the related hyperparameters and the formulation of an algorithm for optimal placement of RBFs in the parameter space as well as automated order selection are still open issues. Progress in this direction will be documented in a future report.

The main emphasis of this work has been on stability and not passivity enforcement. Dedicated algorithms are available for building guaranteed passive parameterized models (for physically passive structures, for which this is appropriate), as far as the number of independent parameters is limited to few units. We refer the Reader to [6], [31], [33], [35], [36], [42], [44]–[47], [49] When the number of parameters increases, there are currently no robust and efficient algorithms for checking and enforcing passivity uniformly in the parameter space. This is still an open problem, and the subject deserves further research efforts by the macromodeling community.

VIII. Acknowledgements

The Authors are grateful to Prof. Manfredi for providing full details on the LNA example discussed in Sections VI-C-VI-D.

Appendix

A. Derivation of Constraints (12)

We show here that constraints (12) provide sufficient conditions for the positive realness of $D(s,\boldsymbol{\vartheta})$. We consider separately the contributions from real and complex conjugate poles in (11).

1) Real poles: Let us consider the n-th basis pole contribution restricted to the imaginary axis $s=\mathrm{j}\omega$, which we rewrite as

$$D_n^r(\mathrm{j}\omega,\boldsymbol{\vartheta})=\frac{r_n(\boldsymbol{\vartheta})}{\mathrm{j}\omega-q_n}, \tag{20}$$

with $q_n\in\mathbb{R}$ and $q_n<0$, and where

$$r_n(\boldsymbol{\vartheta})=\sum_{\ell=1}^{\bar{\ell}} r_{n,\ell}\xi_\ell(\boldsymbol{\vartheta}). \tag{21}$$

Since $\xi_\ell(\boldsymbol{\vartheta})$ and $r_{n,\ell}$ are real-valued, we have

$$\Re\left\{D_n^r(\mathrm{j}\omega,\boldsymbol{\vartheta})\right\}=r_n(\boldsymbol{\vartheta})\cdot\frac{-q_n}{q_n^2+\omega^2}. \tag{22}$$

The first row in constraints (12) states $r_{n,\ell}>0$ for all $\ell=1,\ldots,\bar{\ell}$. Since $\xi_\ell(\boldsymbol{\vartheta})\geq 0$, this implies that $r_n(\boldsymbol{\vartheta})>0$ for all $\boldsymbol{\vartheta}$ and consequently

$$\Re\left\{D_n^r(\mathrm{j}\omega,\boldsymbol{\vartheta})\right\}>0\quad\forall\omega,\ \forall\boldsymbol{\vartheta}. \tag{23}$$

2) Complex poles: Let us consider the contribution from the n-th complex poles pair in (11), restricted to the imaginary axis $s=\mathrm{j}\omega$, which we write as

$$D_n^c(\mathrm{j}\omega,\boldsymbol{\vartheta})=\sum_{\ell=1}^{\bar{\ell}} d_{n,\ell}^c\,\xi_\ell(\boldsymbol{\vartheta}), \tag{24}$$

where

$$d_{n,\ell}^c=\frac{r'_{n,\ell}+\mathrm{j}r''_{n,\ell}}{\mathrm{j}\omega-\alpha_n-\mathrm{j}\beta_n}+\frac{r'_{n,\ell}-\mathrm{j}r''_{n,\ell}}{\mathrm{j}\omega-\alpha_n+\mathrm{j}\beta_n} \tag{25}$$

and where $\alpha_n<0$. We have

$$\Re\{D_n^c(\mathrm{j}\omega,\boldsymbol{\vartheta})\}=\frac{1}{2}\sum_{\ell=1}^{\bar{\ell}}\left[d_{n,\ell}^c+(d_{n,\ell}^c)^*\right]\,\xi_\ell(\boldsymbol{\vartheta}) \tag{26}$$

which is nonnegative provided that

$$d_{n,\ell}^c+(d_{n,\ell}^c)^*>0. \tag{27}$$

Direct evaluation of this expression leads to the following equivalent condition

$$(\alpha_n^2+\beta_n^2)(-r'_{n,\ell}\alpha_n+r''_{n,\ell}\beta_n)+\omega^2(-r'_{n,\ell}\alpha_n-r''_{n,\ell}\beta_n)>0 \tag{28}$$

which is verified when the second row in (12) holds.

3) Superposition: Combining now all individual terms in (11), we see that constraints (12) imply

$$\Re\{D(\mathrm{j}\omega, \boldsymbol{\vartheta})\} > 0 \quad \forall\omega,\ \forall\boldsymbol{\vartheta} \tag{29}$$

since obtained as superposition of nonnegative terms. Using now the minimum principle of analytic functions, we conclude that the analytic function $D(s, \boldsymbol{\vartheta})$ has a nonnegative real part for $\Re\{s\} \geq 0$, since the minimum real part is attained on the imaginary axis $s = \mathrm{j}\omega$.

REFERENCES

[1] S. De Ridder, D. Deschrijver, P. Manfredi, T. Dhaene, and D. V. Ginste, "Generation of stochastic interconnect responses via gaussian process latent variable models," *IEEE Transactions on Electromagnetic Compatibility*, vol. 61, no. 2, pp. 582–585, April 2019.

[2] M. Swaminathan and A. E. Engin, *Power integrity modeling and design for semiconductors and systems*. Prentice Hall Press, 2007.

[3] B. Young, *Digital signal integrity: modeling and simulation with interconnects and packages*. Prentice Hall, 2000.

[4] C. R. Paul, *Introduction to Electromagnetic Compatibility*. Wiley, 1992.

[5] ——, *Analysis of multiconductor transmission lines*. Wiley-IEEE Press, 2008.

[6] S. Grivet-Talocia and B. Gustavsen, *Passive macromodeling: Theory and applications*. John Wiley & Sons, 2015, vol. 239.

[7] S. B. Olivadese, G. Signorini, S. Grivet-Talocia, and P. Brenner, "Parameterized and dc-compliant small-signal macromodels of rf circuit blocks," *IEEE Transactions on Components, Packaging and Manufacturing Technology*, vol. 5, no. 4, pp. 508–522, 2015.

[8] W. H. A. Schilders, H. A. Van Der Vorst, and J. Rommes, *Model order reduction: theory, research aspects and applications*. Springer Verlag, 2008.

[9] Y. Yue, L. Feng, and P. Benner, "Interpolation of reduced-order models based on modal analysis," in *2018 IEEE MTT-S International Conference on Numerical Electromagnetic and Multiphysics Modeling and Optimization (NEMO)*, 2018, pp. 1–4.

[10] A. C. Rodriguez and S. Gugercin, "The p-aaa algorithm for data driven modeling of parametric dynamical systems," *arXiv preprint arXiv:2003.06536*, 2020.

[11] A. Antoulas, A. Ionita, and S. Lefteriu, "On two-variable rational interpolation," *Linear Algebra and its Applications*, vol. 436, no. 8, pp. 2889 – 2915, 2012.

[12] Y. Q. Xiao, S. Grivet-Talocia, P. Manfredi, and R. Khazaka, "A novel framework for parametric loewner matrix interpolation," *IEEE Transactions on Components, Packaging and Manufacturing Technology*, vol. 9, no. 12, pp. 2404–2417, 2019.

[13] S. Grivet-Talocia, "Package macromodeling via time-domain vector fitting," *IEEE Microwave and wireless components letters*, vol. 13, no. 11, pp. 472–474, 2003.

[14] E. J. Grimme, "Krylov projection methods for model reduction," Ph.D. thesis, Univ. Illinois Urbana Champaign, Tech. Rep., 1997.

[15] A. Odabasioglu, M. Celik, and L. T. Pileggi, "PRIMA: Passive reduced-order interconnect macromodeling algorithm," *IEEE transactions on computer-aided design of integrated circuits and systems*, vol. 17, no. 8, pp. 645–654, 1998.

[16] D. L. Boley, "Krylov space methods on state-space control models," *Circuits, Systems, and Signal Processing*, vol. 13, no. 6, pp. 733–758, 1994.

[17] B. Moore, "Principal component analysis in linear systems: Controllability, observability, and model reduction," *Automatic Control, IEEE Transactions on*, vol. 26, no. 1, pp. 17–32, feb 1981.

[18] T. Reis and T. Stykel, "PABTEC: Passivity-preserving balanced truncation for electrical circuits," *Computer-Aided Design of Integrated Circuits and Systems, IEEE Transactions on*, vol. 29, no. 9, pp. 1354–1367, 2010.

[19] K. Glover, "All optimal Hankel-norm approximations of linear multivariable systems and their L_∞ error bounds," *International Journal of Control*, vol. 39, no. 6, pp. 1115–1193, 1984.

[20] D. F. Enns, "Model reduction with balanced realizations: An error bound and a frequency weighted generalization," in *Decision and Control, 1984. The 23rd IEEE Conference on*, Dec 1984, pp. 127–132.

[21] P. Benner, M. Hinze, and E. J. W. ter Maten, *Model reduction for circuit simulation*. Springer, 2010, vol. 74.

[22] B. Nouri, M. S. Nakhla, and X. Deng, "Stable model-order reduction of active circuits," *IEEE Transactions on Components, Packaging and Manufacturing Technology*, vol. 7, no. 5, pp. 710–719, May 2017.

[23] B. Nouri and M. S. Nakhla, "Efficient time-domain sensitivity analysis of active networks," *IEEE Transactions on Components, Packaging and Manufacturing Technology*, vol. 9, no. 9, pp. 1721–1729, Sep. 2019.

[24] D. Deschrijver, L. Knockaert, and T. Dhaene, "A barycentric vector fitting algorithm for efficient macromodeling of linear multiport systems," *IEEE Microwave and Wireless Components Letters*, vol. 23, no. 2, pp. 60–62, Feb 2013.

[25] A. C. Antoulas and B. D. O. Anderson, "On the scalar rational interpolation problem," *IMA Journal of Mathematical Control and Information*, vol. 3, no. 2-3, pp. 61–88, 1986.

[26] S. Lefteriu and A. C. Antoulas, "Modeling multi-port systems from frequency response data via tangential interpolation," in *Signal Propagation on Interconnects, 2009. SPI '09. IEEE Workshop on*, may 2009, pp. 1–4.

[27] A. C. Antoulas, *Approximation of large-scale dynamical systems*. Society for Industrial and Applied Mathematics, 2005.

[28] D. Deschrijver, T. Dhaene, and D. De Zutter, "Robust parametric macromodeling using multivariate orthonormal vector fitting," *IEEE Transactions on Microwave Theory and Techniques*, vol. 56, no. 7, pp. 1661–1667, July 2008.

[29] P. Triverio, S. Grivet-Talocia, and M. S. Nakhla, "A parameterized macromodeling strategy with uniform stability test," *IEEE Trans. Advanced Packaging*, vol. 32, no. 1, pp. 205–215, Feb 2009.

[30] S. Boyd, V. Balakrishnan, and P. Kabamba, "A bisection method for computing the H_∞ norm of a transfer matrix and related problems," *Mathematics of Control, Signals and Systems*, vol. 2, no. 3, pp. 207–219, 1989.

[31] S. Grivet-Talocia, "Passivity enforcement via perturbation of Hamitonian matrices," *IEEE Trans. Circuits and Systems I: Fundamental Theory and Applications*, vol. 51, no. 9, pp. 1755–1769, September 2004.

[32] R. Alam, S. Bora, M. Karow, V. Mehrmann, and J. Moro, "Perturbation theory for Hamiltonian matrices and the distance to bounded-realness," *SIAM J. Matrix Analysis Applications*, vol. 32, no. 2, pp. 484–514, 2011.

[33] Z. Zhang and N. Wong, "Passivity check of S-parameter descriptor systems via S-parameter generalized Hamiltonian methods," *Advanced Packaging, IEEE Transactions on*, vol. 33, no. 4, pp. 1034–1042, Nov 2010.

[34] ——, "An efficient projector-based passivity test for descriptor systems," *Computer-Aided Design of Integrated Circuits and Systems, IEEE Transactions on*, vol. 29, no. 8, pp. 1203–1214, Aug 2010.

[35] S. Grivet-Talocia, "A perturbation scheme for passivity verification and enforcement of parameterized macromodels," *IEEE Transactions on Components, Packaging and Manufacturing Technology*, vol. 7, no. 11, pp. 1869–1881, 2017.

[36] A. Zanco, S. Grivet-Talocia, T. Bradde, and M. De Stefano, "Enforcing passivity of parameterized lti macromodels via hamiltonian-driven multivariate adaptive sampling," *IEEE Transactions on Computer-Aided Design of Integrated Circuits and Systems*, vol. 39, no. 1, pp. 225–238, 2018.

[37] S. Grivet-Talocia and R. Trinchero, "Behavioral, parameterized, and broadband modeling of wired interconnects with internal discontinuities," *IEEE Transactions on Electromagnetic Compatibility*, vol. 60, no. 1, pp. 77–85, 2018.

[38] A. Zanco, S. Grivet-Talocia, T. Bradde, and M. De Stefano, "On stabilization of parameterized macromodeling," in *2019 IEEE 23rd Workshop on Signal and Power Integrity (SPI)*. IEEE, 2019, pp. 1–4.

[39] A. Zanco and S. Grivet-Talocia, "High-dimensional parameterized macromodeling with guaranteed stability," in *2019 IEEE 28th Conference on Electrical Performance of Electronic Packaging and Systems (EPEPS), Montreal (Canada), 6–9 Oct.*, 2019, pp. 1–3.

[40] B. Gustavsen and A. Semlyen, "Rational approximation of frequency domain responses by vector fitting," *Power Delivery, IEEE Transactions on*, vol. 14, no. 3, pp. 1052–1061, jul 1999.

[41] C. Sanathanan and J. Koerner, "Transfer function synthesis as a ratio of two complex polynomials," *Automatic Control, IEEE Transactions on*, vol. 8, no. 1, pp. 56–58, jan 1963.

[42] S. Grivet-Talocia and A. Ubolli, "Passivity enforcement with relative error control," *IEEE Trans. Microwave Theory and Techniques*, vol. 55, no. 11, pp. 2374–2383, November 2007.

[43] E. Fevola, A. Zanco, S. Grivet-Talocia, T. Bradde, and M. De Stefano, "An adaptive sampling process for automated multivariate macromodeling based on hamiltonian-based passivity metrics," *IEEE Transactions on Components, Packaging and Manufacturing Technology*, vol. 9, no. 9, pp. 1698–1711, Sep. 2019.

[44] F. Ferranti, T. Dhaene, and L. Knockaert, "Compact and passive parametric macromodeling using reference macromodels and positive interpolation operators," *Components, Packaging and Manufacturing Technology, IEEE Transactions on*, vol. 2, no. 12, pp. 2080–2088, Dec 2012.

[45] F. Ferranti, L. Knockaert, and T. Dhaene, "Guaranteed passive parameterized admittance-based macromodeling," *Advanced Packaging, IEEE Transactions on*, vol. 33, no. 3, pp. 623–629, Aug 2010.

[46] ——, "Parameterized S-parameter based macromodeling with guaranteed passivity," *Microwave and Wireless Components Letters, IEEE*, vol. 19, no. 10, pp. 608–610, Oct 2009.

[47] ——, "Passivity-preserving parametric macromodeling by means of scaled and shifted state-space systems," *IEEE Transactions on Microwave Theory and Techniques*, vol. 59, no. 10, pp. 2394–2403, 2011.

[48] S. Grivet-Talocia and E. Fevola, "Compact parameterized black-box modeling via fourier-rational approximations," *IEEE Transactions on Electromagnetic Compatibility*, vol. 59, no. 4, pp. 1133–1142, 2017.

[49] E. R. Samuel, L. Knockaert, F. Ferranti, and T. Dhaene, "Guaranteed passive parameterized macromodeling by using sylvester state-space realizations," *IEEE Transactions on Microwave Theory and Techniques*, vol. 61, no. 4, pp. 1444–1454, 2013.

[50] B. D. O. Anderson and S. Vongpanitlerd, *Network analysis and synthesis*. Prentice-Hall, 1973.

[51] M. R. Wohlers, *Lumped and Distributed Passive Networks*. Academic press, 1969.

[52] P. Manfredi and S. Grivet-Talocia, "Rational polynomial chaos expansions for the stochastic macromodeling of network responses," *IEEE Transactions on Circuits and Systems I: Regular Papers*, vol. 67, no. 1, pp. 225–234, Jan 2020.

[53] J. Vlach and K. Singhal, *Computer methods for circuit analysis and design*. Springer, 1983.

[54] S.-H. Min and M. Swaminathan, "Construction of broadband passive macromodels from frequency data for simulation of distributed interconnect networks," *Electromagnetic Compatibility, IEEE Transactions on*, vol. 46, no. 4, pp. 544–558, Nov 2004.

[55] S. Bernstein, "Démonstration du théorème de Weierstrass fondée sur le calcul des probabilités," *Communications de la Société mathématique de Kharkow. 2-ée série*, vol. 13, no. 1, pp. 1–2, 1912.

[56] G. Farin, *Curves and surfaces for computer-aided geometric design: a practical guide*. Academic Press, 1988.

[57] S. Grivet-Talocia and A. Tabacco, "Wavelets on the interval with optimal localization," *Mathematical Models and Methods in Applied Sciences*, vol. 10, pp. 441–462, 2000.

[58] R. Schaback, "A practical guide to radial basis functions," University of Göttingen, Tech. Rep., 2007. [Online]. Available: https://num.math.uni-goettingen.de/schaback/teaching/sc.pdf

[59] D. Wirtz, N. Karajan, and B. Haasdonk, "Surrogate modeling of multiscale models using kernel methods," *International Journal for Numerical Methods in Engineering*, vol. 101, no. 1, pp. 1–28, 2015.

[60] R. Trinchero, M. Larbi, H. M. Torun, F. G. Canavero, and M. Swaminathan, "Machine learning and uncertainty quantification for surrogate models of integrated devices with a large number of parameters," *IEEE Access*, vol. 7, pp. 4056–4066, 2018.

[61] M. Mongillo, "Choosing basis functions and shape parameters for radial basis function methods," *SIAM undergraduate research online*, vol. 4, pp. 190–209, 2011.

[62] S. Grivet-Talocia, S. B. Olivadese, G. Signorini, and P. Brenner, "Compact parameterized macromodels for signal and power integrity analysis of rf and mixed signal systems," in *2013 IEEE Electrical Design of Advanced Packaging Systems Symposium (EDAPS)*. IEEE, 2013, pp. 40–43.

[63] P. Manfredi, D. V. Ginste, D. De Zutter, and F. G. Canavero, "Uncertainty assessment of lossy and dispersive lines in spice-type environments," *IEEE Transactions on Components, Packaging and Manufacturing Technology*, vol. 3, no. 7, pp. 1252–1258, 2013.

[64] T. Buss, "2ghz low noise amplifier with the bfg425w," Philips Semiconductors, B.V., Nijmegen, The Netherlands, Tech. Rep., 1996. [Online]. Available: http://application-notes.digchip.com/004/4-7999.pdf

[65] M. D. McKay, R. J. Beckman, and W. J. Conover, "Comparison of three methods for selecting values of input variables in the analysis of output from a computer code," *Technometrics*, vol. 21, no. 2, pp. 239–245, 1979.

Alessandro Zanco received the Bachelor Degree in Electrical Engineering in 2015 and the Master degree in Mechathronic Engineering in 2018 from Politecnico di Torino, Torino, Italy. He is currently pursuing his Ph.D in Electrical, Electronics and Communication Engineering, at Politecnico di Torino. His research interests include high-dimensional parameterized black-box modeling for EMC.

He is co-recipient of the 2018 Best Paper Award of the IEEE INTERATIONAL SYMPOSIUM ON ELECTROMAGNETIC COMPATIBILITY and of the 2019 Best Student Paper of the IEEE WORKSHOP ON SIGNAL AND POWER INTEGRITY

Stefano Grivet-Talocia (M'98–SM'07–F'18) received the Laurea and Ph.D. degrees in electronic engineering from the Politecnico di Torino, Turin, Italy.

From 1994 to 1996, he was with the NASA/Goddard Space Flight Center, Greenbelt, MD, USA. He is currently a Full Professor of electrical engineering with the Politecnico di Torino. He co-founded the academic spinoff company IdemWorks in 2007, serving as the President until its acquisition by CST in 2016. He has authored over 180 journal and conference papers. His current research interests include passive macromodeling of lumped and distributed interconnect structures, model-order reduction, modeling and simulation of fields, circuits, and their interaction, wavelets, time-frequency transforms, and their applications.

Dr. Grivet-Talocia was a co-recipient of the 2007 Best Paper Award of the IEEE TRANSACTIONS ON ADVANCED PACKAGING. He received the IBM Shared University Research Award in 2007, 2008, and 2009. He was an Associate Editor of the IEEE TRANSACTIONS ON ELECTROMAGNETIC COMPATIBILITY from 1999 to 2001 and He is currently serving as Associate Editor for the IEEE TRANSACTIONS ON COMPONENTS, PACKAGING AND MANUFACTURING TECHNOLOGY. He was the General Chair of the 20th and 21st IEEE Workshops on Signal and Power Integrity (SPI2016 and SPI2017).

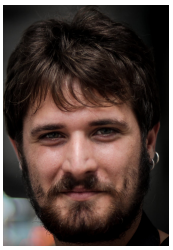

Tommaso Bradde received the Bachelor degree in Electronic Engineering from the Università degli studi Roma Tre, Rome ,Italy, in 2015 and the master degree in Mechatronic Engineering at Politecnico di Torino, Turin, Italy, in 2018. He is currently a Ph.D. student in Electrical, Electronics and Communication Engineering within the Politecnico di Torino. His current research is focused on data-driven parameterized macromodeling.

He is co-recipient of the 2018 Best Paper Award of the IEEE INTERATIONAL SYMPOSIUM ON ELECTROMAGNETIC COMPATIBILITY and of the 2019 Best Student Paper of the IEEE WORKSHOP ON SIGNAL AND POWER INTEGRITY

Marco De Stefano received the M.Sc. degree in mechatronic engineering from Politecnico di Torino, Torino, Italy, in 2018. He is currently pursuing his Ph.D. in Electrical, Electronics and Communication Engineering at the Politecnico di Torino. His research interests include model-order reduction, with emphasis on parameterized macromodeling, and fast simulation methods for signal and power integrity.

He is co-recipient of the 2018 Best Paper Award of the IEEE INTERATIONAL SYMPOSIUM ON ELECTROMAGNETIC COMPATIBILITY and of the 2019 Best Student Paper of the IEEE WORKSHOP ON SIGNAL AND POWER INTEGRITY